

# Three Dimensional CFD Simulations of Two Row Plain Fin and Tube and Heat Exchanger

<sup>1</sup>Rahul Singh, <sup>2</sup>Amol Tripathi

<sup>1,2</sup>RIT COLLEGE, RATAHARA BYPASS REWA 486001 M.P.,INDIA

**ABSTRACT :** Three-dimensional CFD recreations are done to research heat move and liquid stream attributes of a two-line plain balance and-cylinder heat exchanger utilizing ANSYS FLUENT. Warmth move and pressing factor drop qualities of the warmth exchanger are examined for Reynolds numbers going from 330 to 7200. Model math is made, fit, determined, and post-handled utilizing ANSYS Workbench. Liquid stream and warmth move are recreated and results thought about utilizing both laminar and fierce stream models (k-epsilon, and SST k-omega), with consistent state solvers to ascertain pressure drop, stream, and temperature fields. Model approval is done by looking at the recreated case contact factor  $f$  and Colburn  $j$  factor with trial results from the writing. For erosion factor assurance, little distinction is found between the stream models reenacting laminar stream, while in momentary stream, the laminar stream model delivered the most exact outcomes and the k-omega SST disturbance model was more precise in fierce stream systems. The aftereffects of reproductions for heat move in laminar stream utilizing the laminar stream model are discovered to be in acceptable concurrence with the test results, while heat move in temporary stream is best addressed with the SST k-omega chopiness model, and warmth move in tempestuous stream is all the more precisely reenacted with the k-epsilon disturbance model. Sensible arrangement is found between the reproductions and trial information, and the ANSYS FLUENT programming has been adequate for mimicking the stream fields in cylinder blade heat exchangers.

**KEY WORDS:** HEAT EXCHANGER, FIN & TUBE, CFD, ANSYS FLUENT , TRANSITIONAL FLOW, FLUID FLOW

## 1. INTRODUCTION

Fin-and-tube heat exchangers are widely utilized in substance designing, refrigeration, and HVAC (warming, ventilation and cooling) applications, for example, blower intercoolers, air-coolers and fan loops. The plate blade and-cylinder heat exchangers, comprising of precisely or powerfully extended round cylinders in a square of equal consistent balances, are broadly utilized in industry and

especially in the warming, cooling and refrigeration businesses. The predominant warm obstruction is for the most part on the air side in pragmatic applications, and subsequently the utilization of finned surfaces on the air side is basic to adequately improve the general warm presentation of warmth exchangers. These finned surfaces incorporate creased twisting balance, plain balance, cut blade and balance with delta-wing longitudinal vortex generator, etc. Regardless of these, upgraded blade surfaces can essentially improve the warmth move coefficients in examination with their plain balance partner, the plain balance is still by a wide margin the most famous balance design utilized noticeable all around cooled heat exchangers. This is a result of its boss dependability under long haul activity and its lower grinding attributes.

### 1.1 PROBLEM FORMULATION

For this task, the mathematical boundaries of a two-line heat exchanger dependent on trial research [Wang et al., 1996] are utilized to fabricate a CFD model, and results read from the charts (contact factor and Colburn j-factor against Reynolds number) in the article are utilized to approve the consequences of the CFD reenactments. The boundaries of interest: contact factor  $f$  and Colburn j-factor are broadly utilized in industry to portray pressure drop and warmth move, separately, and consequently decide heat exchanger execution and appropriateness for explicit obligations. Deciding and utilizing these boundaries for execution forecast is essential for the warmth exchanger configuration measure.

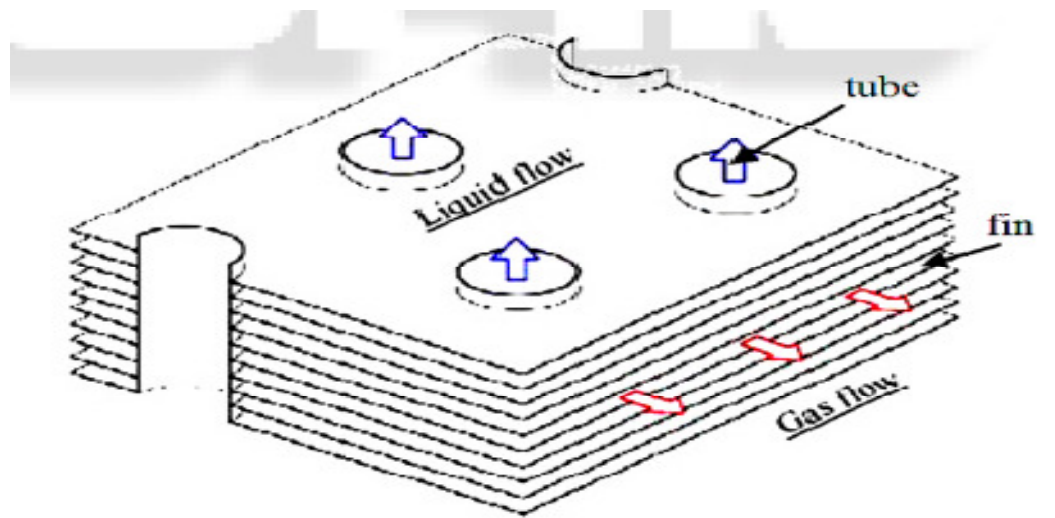


Figure 1 : Typical Fin-and-Tube heat exchanger section with staggered tube arrangement[1]

The two-column balance and-cylinder heat exchanger contemplated has a stunned cylinder plan, as

delineated in Figure 1. Dissecting stream and warmth move utilizing CFD can make counts to anticipate heat exchanger execution simple. Notwithstanding, it is preposterous to expect to perform CFD reenactment on the whole warmth exchanger, because of the huge number of volumes and figuring's required. Accordingly, a little segment of a warmth exchanger comprising of one channel of air between two balances, with the air streaming by two cylinders is demonstrated for this undertaking. Reenactments of the wind stream through this section are done, while applicable qualities of the wind current are examined and arrived at the midpoint of at the inflow, least free-stream area(s), and surge. The attributes inspected are: stream speed (in every one of the three bearings: x, y, and z), temperature and pressing factor. These estimations are then utilized for ascertaining pertinent execution boundaries, for example, pressure drop, rubbing and Colburn factors, heat move rate, Reynolds number and so forth.

## **1.2 PROJECT OUTLINE**

For examination with the charts in the approval research article [Wang et al., 1996], progressions of ten distinctive Reynolds numbers (in light of cylinder collar measurement and least free-stream speed) are reproduced going from around 330 to 7200 with delta frontal air speeds going from 0.3 to 6.2 m/s. Water streams at 60 °C through the cylinders and cold air through the balances. For figuring out which disturbance model most precisely addresses heat exchanger stream and warmth move at the diverse stream systems (laminar, momentary, and violent), three stream models are picked for the recreations. They are: laminar, k-epsilon choppiness model, and SST k-omega disturbance model. A consistent state FLUENT solvers is utilized for the 30 reproductions (1 solvers \* 10 speeds \* 3 stream models). All computational work is done utilizing ANSYS Workbench. Pre-preparing programming Design Modeler is utilized for calculation. Lattice module is utilized for cross section, ANSYS FLUENT CFD solver and CFD post-preparing for perception. Pressing factor drop and warmth move results and correlations of the diverse disturbance models is accounted for and talked about. After this presentation area, the typical important points are covered: a model portrayal of the warmth exchanger to incorporate administering conditions, computational space, and cross section. At that point the exhibition boundaries identified with pressure drop and contact factor are introduced, which is trailed by a segment on computational liquid elements (CFD), including conditions, and arrangement calculation. At last, the outcomes are introduced. The report closes with conversation and end areas.

### **1.3 MODEL DESCRIPTION**

Heat exchangers are utilized for moving nuclear power between liquids, surfaces, or mixes of these, when they are at contrasting temperatures and in warm contact. Commonplace applications incorporate warmth recuperation, sanitization, refining, and warming or cooling of a specific liquid stream. The liquids can be isolated by a divider or in direct contact. In the event that there is a divider going about as the warmth move surface isolating liquids, members, or blades, can be associated with it to build the warmth move surface territory.

#### **A. Classification**

Warmth exchangers can be characterized by development type, stream course of action, or surface conservativeness, among different kinds conceivable. In the event that the arrangement is by development, the sorts of warmth exchangers are: plate, rounded, expanded surface, or regenerative. In the event that characterization is by stream plan, the sorts can incorporate single-pass or multi-pass of counter-stream, equal stream, cross-stream, or blends of stream.

#### **B. Fin-and-Tube Heat Exchangers**

The Fin and Tube heat exchanger (HE) concentrated in this undertaking is named broadened surface, single-pass with cross-stream. This kind of warmth exchanger is broadly utilized in different warm designing applications, including substance plants, food businesses, HVAC, car, airplane, and the sky is the limit from there. They comprise of a square of equal consistent balances with round cylinders precisely or powerfully ventured into the balances, a well known warmth exchanger intended for liquid to stream in the cylinders and gas between the blades (see Figure 1).

The benefits of utilizing more conservative warmth exchangers, for example, the balance and-cylinder are many. The all-encompassing surfaces (blades) are intended to expand the warmth move zone per unit volume, bringing about smaller units of decreased space and weight (up to multiple times more prominent surface territory per unit volume when contrasted with shell-and-cylinder exchangers), with higher warmth move coefficients than other less minimized warmth exchanger types. There is likewise adaptability when planning the surface zone dispersion between the hot and cold sides. Significant expense reserve funds are normal. For touchy materials, more tight temperature control is a favorable position, improving item quality. Various liquid streams can be

obliged. There are likewise restrictions to utilizing balance and-cylinder heat exchangers.

### **C. Typical Materials and Geometry:**

Fines are normally made of aluminum, while tubes are made of copper. Commonplace calculation: blade thickness 0.11 to 0.13 mm, tubes with outside measurement 10 mm, cross over pitch 25 mm, longitudinal pitch 22 mm, and balance thickness of 6 to 16 balances for every inch. (Notwithstanding, more modest cylinder dividing and tube widths are getting more inescapable) .

### **D. Computational Domain**

The pre-processing software ANSYS Design Modeler and Mesh module is used to create and mesh the computational model.

Geometric Parameter	Symbol	Dimensions
Fin Thickness	t	0.130 mm
Fin Pitch	Fp	2.240 mm
Fin collar Outside Diameter	Dc	10.23 mm
Transverse Pitch	Pt	25.40 mm
Longitudinal Pitch	Pl	22.00 mm
Tube Wall Thickness	$\delta$	0.336 mm
Number of Tube Rows		2

**Table 1 : Geometric dimensions of heat exchanger model**

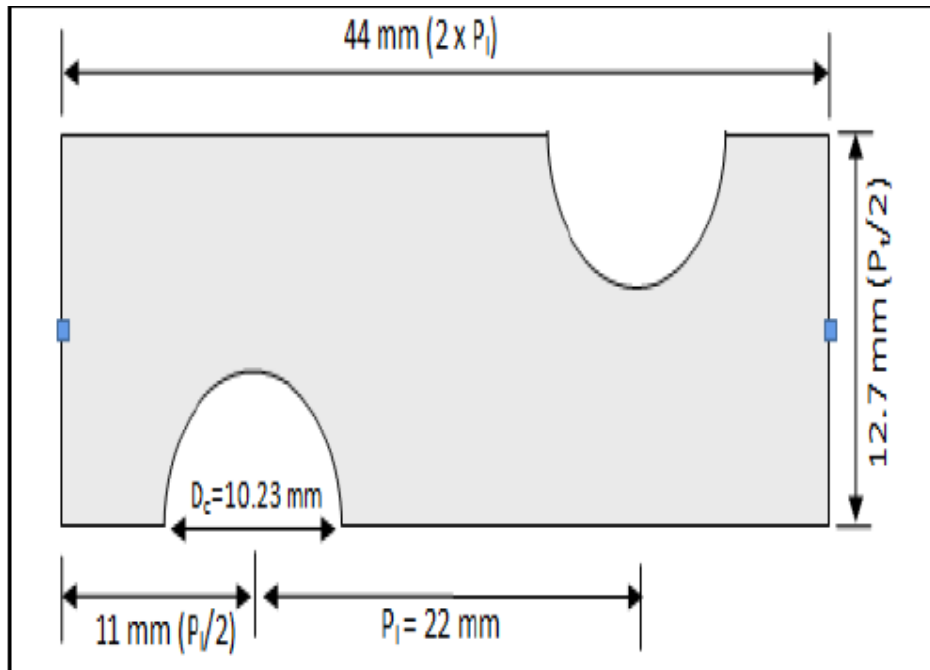


Fig. 2: Illustration of the main computational domain and geometric parameters of the heat exchanger model studied

The computational domain is actually 8 times the original heat transfer area (as illustrated in Figure 2), and is defined by  $0 < x < 8P_1$ ,  $0 < y < P_t/2$ , and  $0 < z < F_p$ , while the actual modeled heat exchanger length is equal to twice the longitudinal pitch  $P_1$ . The volume representing the air which passes through the gap between the two fins is extended upstream from the inlet and downstream from the outlet in order to reduce oscillations and ensure a representative flow in the computational domain of the actual heat exchanger.

### Governing Equations and Numerical Schemes

The governing equations for this project are the three-dimensional continuity, Navier-Stokes for momentum, energy, and scalar transport equations for steady-state flow, and can be written (generally) as follows:

$$\frac{\partial(\rho u_i)}{\partial x_i} = 0 \quad (1)$$

Momentum equation:

$$\frac{\partial}{\partial x_i}(\rho u_i u_j) = \frac{\partial}{\partial x_i} \left( \mu \frac{\partial u_j}{\partial x_i} \right) - \frac{\partial p}{\partial x_j} \quad (2)$$

Energy equation:

$$\frac{\partial}{\partial x_i}(\rho u_i T) = \frac{\partial}{\partial x_i} \left( \frac{k}{C_p} \frac{\partial u_j}{\partial x_i} \right) \quad (3)$$

General transport equation (for scalars):

$$\frac{\partial(\rho u_i \phi)}{\partial x_i} = \frac{\partial}{\partial x_i} \left[ \Gamma_\phi \frac{\partial \phi}{\partial x_i} \right] + S_\phi \quad (4)$$

The general equations 1-3 are used in the CFD computations to calculate the flow field for both thermal and fluid (air) dynamics, solving for heat transfer and pressure drop. They are discretised and solved by the finite volume method. It is solved on a staggered grid using solvers for laminar and turbulent flow, with the latter solution solved using the Reynolds Averaged Navier-Stokes equations (RANS) with both k-epsilon and SST k-omega turbulence models. To ensure coupling between velocity and pressure, the SIMPLE algorithm is used.

#### 1.4 COMPUTATIONAL FLUID DYNAMICS

Computational Fluid elements (CFD) is a PC based recreation strategy for investigating liquid stream, heat move, and related marvels, for example, ignition, substance responses and so on This undertaking utilizes CFD for examination of stream and warmth move. A few instances of utilization zones are: streamlined lift and drag (for example planes or windmill wings), power plant burning, substance measures, warming/ventilation, and even biomedical designing (reproducing blood move through supply routes and veins). CFD investigation did in the different enterprises is utilized in R&D and assembling of airplane, burning motors, just as numerous other mechanical items. It very well may be profitable to utilize CFD over customary test based examination, since tests have an expense straightforwardly corresponding to the quantity of setups wanted for testing, not at all like with CFD, where a lot of results can be delivered at for all intents and purposes no additional cost. Thusly, parametric investigations to streamline gear are reasonable with CFD when contrasted with tests. This part momentarily depicts the overall ideas and hypothesis identified with utilizing CFD to

break down liquid stream and warmth move, as pertinent to this venture. It starts with an audit of the instruments required for completing the CFD investigation and the cycles required, trailed by an outline of the administering conditions.

### **1.5 CFD Computational Tools :**

This segment depicts the CFD instruments needed for completing a reproduction and the cycle one continues to tackle an issue utilizing CFD. The equipment required and the three fundamental components of handling CFD reproductions: the pre-processor, processor, and post-processor are depicted. There is assortment of business CFD programming accessible, for example, ANSYS Fluent, ANSYS CFX, ACE, just as a wide scope of reasonable equipment and related expenses, contingent upon the multifaceted nature of the cross section and size of the computations. Confounded transient cases with fine networks will require more impressive PC processors and RAM than less complex cases with harsh cross sections.

To run a recreation, three primary components are required:

#### **1) Pre-processor:**

A pre-processor is used to define the geometry for the computational domain of interest and generate the mesh of control volumes (for calculations). Generally, the finer the mesh in the areas of large changes the more accurate the solution. Fineness of the grid also determines the computer hardware and calculation time needed. Design Modeler and Mesh tool in ANSYS Workbench are used as pre-processor.

#### **2) Solver:**

The solver makes the estimations utilizing a mathematical arrangement strategy, which can utilize limited contrast, limited component, or ghostly strategies. Most CFD codes utilize limited volumes, which is an extraordinary limited contrast strategy. First the liquid stream conditions are incorporated over the control volumes (bringing about the specific protection of applicable properties for each limited volume), at that point these indispensable conditions are discretised (delivering arithmetical conditions through changing over of the vital liquid stream conditions), lastly an iterative strategy is utilized to settle the mathematical conditions.

#### **Post-Processor:**

The post-processor provides for visualization of the results, and includes the capability to display the



geometry/mesh,

## **2 . Problem-Solving with CFD**

There are numerous choices to be made prior to setting up the issue in the CFD code. A portion of the choices to be made can include: regardless of whether the issue ought to be 2D or 3D, which sort of limit conditions to utilize, regardless of whether to ascertain pressure/temperature varieties dependent on the wind stream thickness, which choppiness model to utilize and so forth The presumptions made ought to be decreased to a level as straightforward as could really be expected, yet as yet holding the main highlights of the issue to be tackled to arrive at a precise arrangement. After the above choices are made, the math and cross section can be made. The matrix ought to be made as fine as needed to make the recreation 'lattice autonomous'. To decide the fineness required, a matrix reliance study is ordinarily completed by making a progression of refinements on an at first course network, and doing reproductions on each to decide when the critical aftereffects of interest don't change, now the framework is viewed as free. To arrive at a combined arrangement, unwinding variables and speeding up gadgets can be picked. At long last, to guarantee exactness of the reenactments, they ought to be approved against test information. These activities recreation results are contrasted with a test study detailed in the writing. Subtleties of the warmth exchanger math, introductory limit conditions identified with stream and temperature were followed as intently as conceivable when fabricating this CFD model.

### **2.1 The SIMPLE Algorithm**

The SIMPLE algorithm is a guess-and-correct technique to determine the values for pressure on a staggered grid. It is iterative and must be done in the specific order when other scalars are also calculated. The general procedure for the technique is shown in Figure 3, which is followed by a description of the steps in the algorithm.

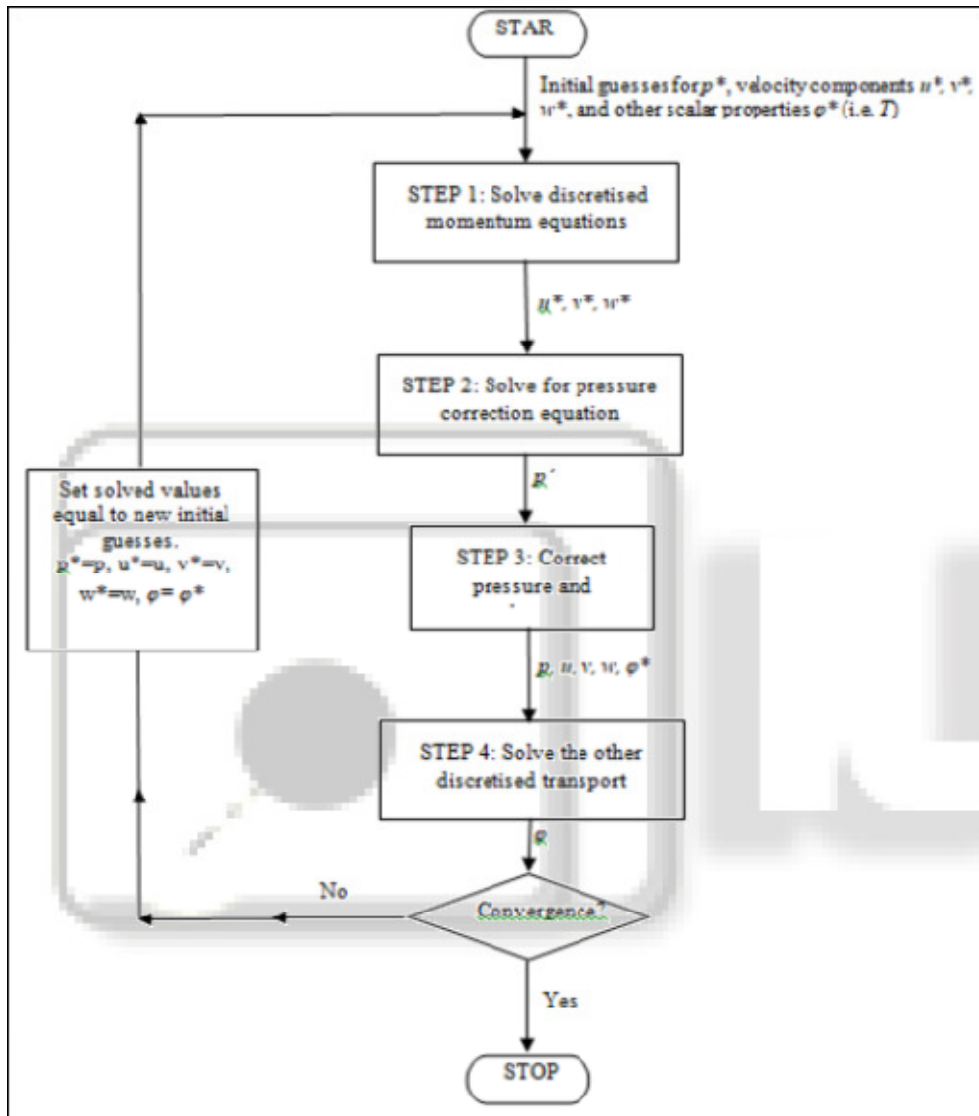


Figure 3 : SIMPLE Algorithm

The steps in the SIMPLE algorithm, as shown in Figure 4.6, are summarized as:

**START**

Estimate a starting guess for the pressure field  $p^*$ .

**1) STEP 1 :**

Solve the discretised momentum equations for the velocity components based on the pressure guess  $p^*$ . For a three-dimensional case as the one in this project, 6 discretised momentum balances are solved for each of the six neighbours for node P (W, E, S, N, B, and T). This step results in finding values for  $u^*$ ,  $v^*$ ,  $w^*$ , based on  $p^*$ .

## **2) STEP 2**

Solve for pressure correction equation to find the pressure correction  $p'$ . This is done with the discretised continuity equation by finding the mass imbalance and between total mass flow inflow and the total mass outflow of the six 'guessed' velocities (calculated based on the guessed pressure  $p^*$ ).

## **3) STEP 3**

Correct the pressure and velocity components using the pressure correction, where the correction ( $p'$ ) is added to the initial guess ( $p^*$ ), to get the new pressure field  $p$ ,

This step of the SIMPLE algorithm results in calculated values for velocity components and pressure:  $p$ ,  $u$ ,  $v$ ,  $w$ ,  $\phi^*$ , after correcting the guesses, which satisfy the continuity equation.

## **4) STEP 4**

Solve the other discretised transport equations using the line-TDMA method to get calculated values for the remaining scalar variables  $\phi$ .

### **1) Convergence**

After step 4, the outputs are tested for convergence (meaning that the mass imbalance is very close to zero), and if this is not within the value required for convergence, the program loops back to the beginning, using the newly calculated pressure, velocity, and other scalar values as the next starting guess. The process continues until convergence occurs (iteration).

### **2) Relaxation Factors**

Often the pressure correction is too large, causing unstable calculations and divergence rather than convergence. Due to this problem, the iteration procedure must be slowed down to under-relax the pressure corrections. This is done by utilizing an under-relaxation factor  $\alpha$  of between 0 and 1, which is multiplied by the correction factor so that only a fraction of the originally calculated correction factor is actually used in the calculation, (for example with the pressure correction): Under-relaxation factors are also used for the velocity components. Oscillatory or divergent solutions are a result of too large values for  $\alpha$ , while very slow convergence results from too small of values for the under-relaxation factor. Therefore, the correct under-relaxation factor is important for a converged solution, but cannot be determined in generation.

### 3. RESULT AND DISCUSSION

#### 3.1 Grid Independence Test:

Grid independence test is used to check how the grid size affects the simulation results. In this test, the same geometric model with different grid sizes is simulated. The mesh which does not alter the simulation result is used as independent grid. This is to minimize the error due to grid size (discretisation error). For this project 5 mesh sizes with 1360, 32850, 44199, 150521 and 275324 cells is simulated to get pressure drop between inlet and outlet. Based on the comparison of simulated results, the grid with 150521 numbers of cells is selected for project, as independent grid size. Even though mesh size with 150521 and 275324 cells gives nearly same result, the one with 150521 cells reduces computational time. Experimental Results

#### 1) Experimental Values for Colburn j-Factor:

The values of the Reynolds number and j-factor as read from the graph in the article (Wang et al. 1996) [1] for the specific heat exchanger geometry studied in this project are listed in Table 2 and presented in the graph in Figure 4.

Re	Colburn j factor
330	0.042
600	0.027
790	0.023
1300	0.017
1700	0.014
2900	0.012
4300	0.0094
5200	0.009
6200	0.0084
7200	0.0081

Table 2 : Experimental values for Colburn j- factor

It can be seen in Table 2 and Figure 4 that the Colburn j-factor decreases with increasing Reynolds number. It ranges from 0.042 at the lowest Reynolds number to 0.0081 at the high Reynolds number. A plot of this type (j vs. Re) for a typical circular tube normally have a more distinct dip in the transition region than in this graph for air flow through a heat exchanger. However, a slight change is seen at Reynolds number 1300, and the graph appears to level off again at Reynolds number 2900. It can therefore be determined from this graph that the laminar flow region goes up to around Reynolds number 1300 (it is difficult to determine exactly without more data points), with a transition region

after that, and the turbulent flow begins at a point around Reynolds number 2900. Values for the Colburn j-factor determined from simulations, and followed by the appropriate calculations for this project are compared to these experimental values. During the comparisons, it is kept in mind that the uncertainties in the Colburn j-factor values (experimentally determined values) can be high for the lower Reynolds numbers (uncertainty is  $\pm 9.4\%$  at Reynolds number 600, and may be even higher at Reynolds number 330, the value of which was not provided in the article).

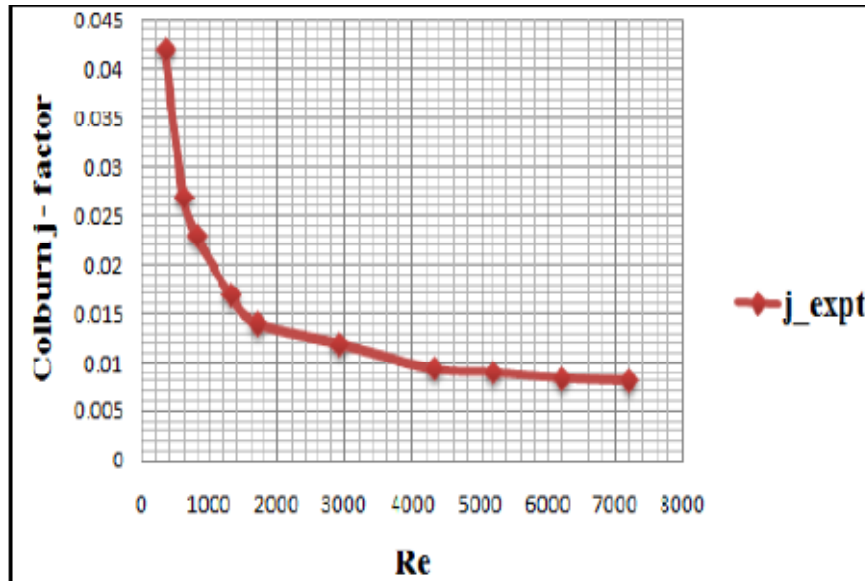


Figure 4 : Plot of Reynolds Number Vs Colburn j- factor, determined experimentally

## 2) Experimental Values for Fanning Friction Factor $f$

To validate the pressure-loss simulations in this project, the Fanning friction factor  $f$  determined experimentally from Wang et al. (1996) are used. The values for Reynolds number and friction factor  $f$  as read from the graph in the article for the specific heat exchanger geometry studied in this project are listed in Table 3 and presented in the graph in Figure 5.

Re	Friction factor f
330	0.11
600	0.073
790	0.063
1300	0.046
1700	0.042
2900	0.033
4300	0.027
5200	0.024
6200	0.022
7200	0.021

Table 3 : Experimental values for Fanning friction factor f

It can be seen in Table 3 and Figure 5 that like the Colburn j-factor, the Fanning friction factor f also decreases as the Reynolds number increases. It ranges from 0.11 at the lowest Reynolds number to 0.021 at the high Reynolds number. A slight change can be seen at Reynolds number 1300, and the graph levels off again between Reynolds number 1300 and 1700. It can therefore be determined from this graph that the laminar flow region goes up around Reynolds number 1300, with a transition region thereafter, and from the slight change in graph again, the turbulent flow regime seems to begin at around Reynolds number 1700 (or possibly it is closer to 2900 since that is what was found on the j-factor graph). However, more data points would be necessary to accurately determine the critical Reynolds values for the different flow regimes. Values for the friction factor f as calculated from the pressure drop values of the simulations are compared to the experimental values from Wang et al. (1996) [1]. During the comparisons, it is kept in mind that the uncertainties in the Fanning friction factor f values (experimentally determined values) can be high for the lower Reynolds numbers (the uncertainty is given as  $\pm 17.7\%$  at Reynolds number 600, and may be even higher at Reynolds number 330, the value of which was not provided in the article.)

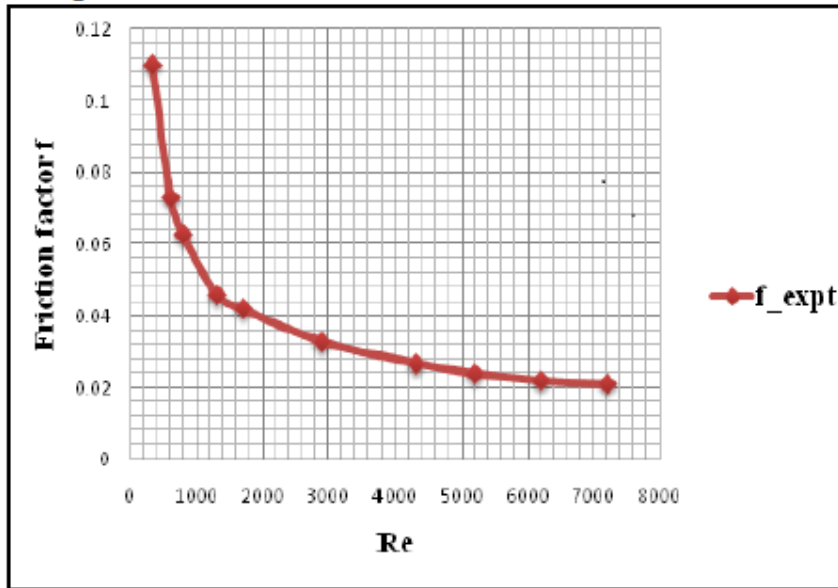


Figure 5 : Plot of Reynolds Number Vs Fanning friction factor f, determined experimentally

#### A. Characteristics of Flow

This section describes the observations found using CFD Post after running the CFD simulations in ANSY Fluent. The characteristics of low-Reynolds flow and high-Reynolds flow are compared with contour plots of velocity with vectors.

#### 3.2 Comparison of Numerical and Experimental Results

Simulation is carried out using ANSYS fluent for different flow model as described in section 1.2. Pressure drop, maximum velocity and heat transfer coefficient data is recorded for 10 inflow velocities. Based on these recorded values friction factor and Coburn j-factor is calculated. Fanning friction factor f is tabulated in Table 4 and plotted in Figure 6 against Reynolds number to compare with experimental values. It is clear from graph that simulated values follows the same trend as experimental values. Figure 7 shows the percent error in the simulated values with respect to experimental values of friction factor f.

Re	Fanning friction factor $f$ (Numerical Results)		
	Laminar	k-epsilon	SST k-omega
330	0.114301	0.12834	0.11573
600	0.078958	0.085486	0.081130
790	0.063243	0.066578	0.066373
1300	0.049123	0.048782	0.053733
1700	0.042439	0.040209	0.046074
2900	0.033973	0.030271	0.034262
4300	0.028998	0.025240	0.028268
5200	0.027105	0.023353	0.025690
6200	0.025445	0.022123	0.023610
7200	0.024416	0.021219	0.022234

Table 4: Fanning friction factor  $f$  (Numerical Results)

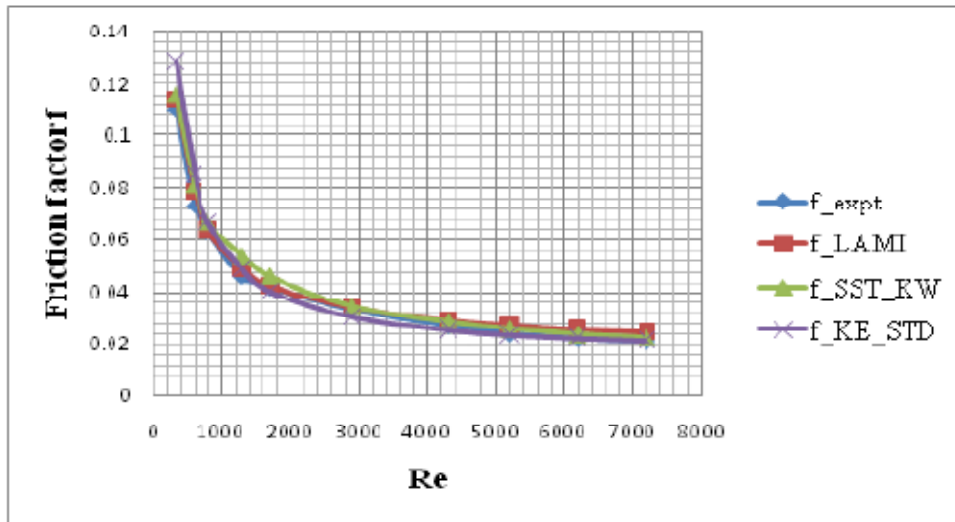


Figure 6: Comparison of experimental and numerical values for friction factor  $f$



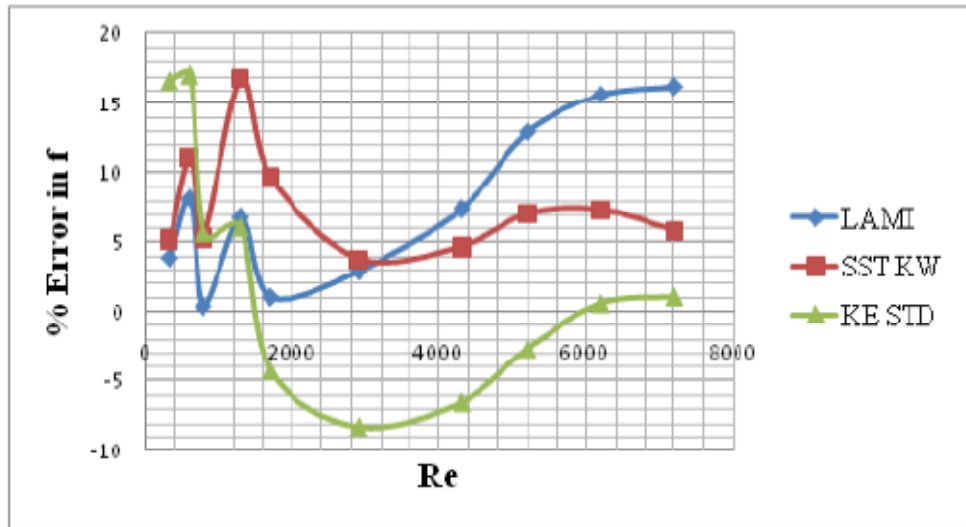


Figure 7: Percentage error in friction factor f

In the same manner the Colburn j-factor is tabulated and compared with experimental value. Finally, percent error is plotted for simulated values with respect to experimental values.

Re	Colburn j factor (Numerical Result)		
	Laminar	k-epsilon	SST k-omega
330	0.034964	0.039524	0.035225
600	0.027451	0.032419	0.027989
790	0.023432	0.027021	0.024140
1300	0.018764	0.021256	0.020222
1700	0.015851	0.017826	0.017801
2900	0.011650	0.012691	0.013595
4300	0.008790	0.009822	0.010913
5200	0.007840	0.008457	0.009719
6200	0.006792	0.007277	0.008869
7200	0.005960	0.006512	0.007978

Table 5: Colburn j-factor (Numerical Results)

#### **4. CONCLUSION**

The goal of this venture is to build up the CFD reproduction model for two-column blade and-cylinder heat exchanger and confirm the consequences of reenactment with the accessible test information from the writing. The motivation behind the work was to research the prospects of at last utilizing CFD computations for plan of warmth exchangers rather than costly test testing and model creation. To dissect the stream and warmth move qualities of the warmth exchanger, a model of a two-column blade and-cylinder heat exchanger is made utilizing Design modeler and Mesh module to make the math and cross section individually. The subsequent lattice (after a framework freedom test was done) is utilized for running reproductions utilizing a laminar stream model and two turbulence models. Ten diverse delta stream speeds going from 0.3 m/s to 6.2 m/s and relating to Reynolds numbers going from 330 to 7200 are recreated in the three distinctive stream models (laminar, k-epsilon disturbance model, and SST k-omega choppiness model). Utilizing the recreation results computations identified with heat stream and pressing factor misfortune are done to decide the Fanning contact factor  $f$  and Colburn  $j$ -factor for examination with the writing esteems utilized for the approval. It is discovered that the stream model exactness relied upon the stream system and whether the erosion factor  $f$  or  $j$ -factor is being resolved. From the test esteems given in the writing, the laminar stream district for this specific calculation of warmth exchanger changed to temporary at around Reynolds number 1300, and moving to fierce around Reynolds number 2900. The Reynolds number has a trademark measurement of the cylinder collar outside width. For contact factor assurance, little distinction is found between the stream model recreating laminar stream, while in temporary stream, the laminar stream model created the most precise outcomes (for grinding factor) and the SST k-omega disturbance model is more exact in fierce stream systems. For heat move, the laminar stream model figures the most precise  $j$ -factor, while for temporary stream the SST k-omega choppiness model is more exact and the k-epsilon disturbance model is best for heat move reproductions of violent stream. The stream model can be picked dependent on the thing is being examined (heat stream or pressing factor drop) and the stream system. It tends to be presumed that the pressing factor drop and warmth move qualities of a balance and-cylinder heat exchanger can be resolved with sensible precision utilizing CFD calculations did in ANSYS Workbench. These outcomes can be utilized to do pragmatic work in the plan cycle of warmth exchangers.

#### **REFERENCES**

- [1] Wang, Chi-Chuan; Chang, Yu-Juei; Hsieh, Yi-Chung; Lin, Yur-Tsai. "Sensible heat and friction characteristics of plate fin-and-tube heat exchangers having plane fins", International Journal of Refrigeration, Vol. 19, No. 4 (1996) pp. 223-230.
- [2] Kayansayan, N. "Heat transfer characterization of plate fin-tube heat exchangers", International Journal of Refrigeration, Vol. 17, No. 1 (1994) pp. 49-57.
- [3] Yan, Wei-Mon; Sheen, Pay-Jen. "Heat transfer and friction characteristics of fin-and-tube heat exchangers", Volume 43 (2000), pp. 1651-1659.
- [4] Ay, Herchang; Jang, Jiin Yuh; Yeh, Jer-Nan. "Local heat transfer measurements of plate finned-tube heat exchangers by infrared thermography", International Journal of Heat and Mass Transfer, Vol. 45 (2002), pp. 4069-4078.

- [5] Gray, D. L.; Webb, R.L. "Heat transfer and friction correlations for plate fin-and-tube heat exchangers having plain fins", Proceedings of the Ninth International Heat Transfer Conference, San Francisco (1986).
- [6] Rocha, L. A. O.; Saboya, F. E. M.; Vargas, J. V. C. "A comparative study of elliptical and circular sections in one- and two-row tubes and plate fin heat exchangers", International Journal of Heat and Fluid Flow, Vol. 18 (1997), pp. 247-252.
- [7] Perrotin, Thomas. "Fin efficiency calculation in enhanced fin-and-tube heat exchangers in dry conditions", International Congress of Refrigeration, ICR0026 (2003).
- [8] Chen, Han-Taw; Chou, Juei-Che; Wang, Hung-Chih. "Estimation of heat transfer coefficient on the vertical plate fin of finned-tube heat exchangers for various air speeds and fin spacings", International Journal of Heat and Mass Transfer, Vol. 50 (2006) pp. 45-57.
- [9] Tao, Y. B.; He, Y. L.; Huang, J.; Wu, Z. G.; Tao, W. Q. "Three-dimensional numerical study of wavy fin-and-tube heat exchangers and field synergy principle analysis", International Journal of Heat and Mass Transfer, Vol. 50 (2007), pp. 1163-1175.
- [10] Erek, Aytunc; Özerdem, Baris; Bilir, Levent; Ilken, Zafer. "Effect of geometrical parameters on heat transfer and pressure drop characteristics of plate fin and tube heat exchangers", Applied Thermal Engineering, Vol. 25 (2005) pp. 2421-2431.